E JOURNAL

Process-Induced Aging of Poly(lactic acid) in Additive Manufacturing Using Fused Granular Fabrication

Authors Luca P. M. Bürgel (M. Sc.) [a], Christopher Krüsener (M. Sc.) [b], Dr. Tobias Grimm [a], Prof. Dr. Ulrich A. Handge [b], Prof. Dr. Jan T. Sehrt [b]

[a] **Hybrid Additive Manufacturing (HAM),** Ruhr University Bochum, Universitätsstraße 150, 44801 Bochum, Germany

[b] **Chair of Plastics Technology**, TU Dortmund University, Leonhard-Euler-Str. 5, 44207 Dortmund, Germany

Zusammenfassung Diese Studie bewertet systematisch die Wiederverwertbarkeit von Polylactid (PLA) in der additiven Fertigung mittels granulatbasierter Materialextrusion. Ziel ist die Definition von Akzeptanzbereichen und Leitlinien für die Regranulierung, um höhere Sekundärmaterialanteile und industrietaugliche Recyclingpfade zu ermöglichen. PLA wird in bis zu fünf mechanischen Recyclingzyklen verarbeitet, wobei standardisierte Prüfkörper unter definierten und unveränderten Prozessparametern hergestellt werden. Die Bewertung erfolgt mittels Zugversuchen (DIN EN ISO 527-1), Dreipunktbiegeversuchen (DIN EN ISO 178) sowie oszillatorischer Scherrheologie zur Charakterisierung des Schmelzfließverhaltens und der Materialalterung. Die Wiederverwendung von recyceltem PLA im Fused Granular Fabrication (FGF) Prozess beeinflusst sowohl die Verarbeitbarkeit als auch die Bauteileigenschaften. Die komplexe Viskosität sinkt nach fünf Recyclingzyklen um ca. 40 %, was auf eine verarbeitungsinduzierte Materialalterung hindeutet. Die mechanischen Eigenschaften zeigen Minderungen von 10 bis 40 %, wobei Zug- und Biegemodul nur geringfügige Veränderungen aufweisen. Eine bis zu fünfmalige Verarbeitung von recyceltem PLA ist mittels FGF möglich, was dessen Potenzial für industrielle Anwendungen unterstreicht.

Abstract This study systematically evaluates the recyclability of poly(lactic acid) (PLA) in additive manufacturing via granule-based material extrusion. The objective is to define acceptance ranges and practical guidelines for regranulation, enabling higher secondary material shares and technically robust, industry-ready recycling pathways. PLA is processed through up to five mechanical recycling cycles, with standardized specimens produced under defined and consistent process parameters at each stage. Material characterization is performed using tensile

testing (DIN EN ISO 527-1), three-point bending tests (DIN EN ISO 178), and oscillatory shear rheology to assess melt flow behavior and material degradation. Reprocessing recycled PLA via Fused Granular Fabrication (FGF) affects both processability and final part properties. The complex viscosity decreases by approximately 40% after five recycling cycles, indicating processing-induced material aging. Mechanical properties exhibit reductions of 10–40%, depending on the parameter considered, while Young's modulus and flexural modulus show only minor variations. Overall, recycled PLA can be reprocessed up to five times via FGF, demonstrating its potential for industrial-scale applications.

Key Words Recycling, Poly(lactic acid), Fused Granular Fabrication, Sustainability, Additive Manufacturing, Rheology.

1. Introduction and Motivation

The rapid industrial and societal demand for sustainable materials has stimulated growing research interest in bioplastics such as poly(lactic acid) (PLA), a renewable aliphatic polyester derived from agricultural resources, including corn and sugarcane [1–3]. Historically, the development of plastics has driven technological advancement, but their environmental persistence and the accumulation of plastic waste have spurred the transition towards biodegradable alternatives [4, 1]. PLA has emerged as one of the most promising candidates for reducing dependency on fossil-derived polymers, combining biodegradability, biocompatibility, and mechanical versatility suitable for diverse engineering and biomedical applications [5, 6]. In parallel with the global movement towards circular manufacturing, additive manufacturing (AM) has gained strategic importance for sustainable production. Among the various AM technologies, Fused Granular Fabrication (FGF) stands out for its direct use of polymer granules without filament pre-processing, offering significant advantages in cost, energy efficiency, and recyclability [7, 8]. The integration of FGF and biodegradable polymers like PLA aligns with emerging circular economy principles, enabling closed-loop material cycles through regrinding and reprocessing [9, 10]. However, the mechanical and rheological stability of PLA under repeated thermal and shear stresses during manufacturing and regranulation remains a critical challenge [11, 12]. Despite the broad applicability of PLA, its susceptibility to hydrolytic degradation, chain scission, and crystallization effects under processing and environmental exposure conditions significantly affects its performance [13, 14]. Studies have shown that process-induced aging during extrusion alters molecular weight, crystallinity, and viscoelastic response, leading to property deterioration over time [15, 16]. In the context of FGF, the elevated thermal residence time and potential oxidative conditions introduce additional degradation pathways that may differ substantially from filament-based additive manufacturing [17, 18]. Moreover, as recycled or reclaimed PLA feedstocks are increasingly employed, understanding the relationship between processing history, thermomechanical exposure, and resultant aging phenomena has become a prerequisite for ensuring reproducible quality in large-format extrusion applications [19, 8]. This study aims to investigate the process-induced aging of PLA during FGF focusing on the interplay between processing parameters, thermal history, and material degradation mechanisms. By analyzing morphological, rheological, and mechanical evolution before and after processing, the research seeks to elucidate the cumulative effects of thermo-oxidative and hydrolytic aging introduced during the additive manufacturing workflow. The overarching motivation lies in bridging the gap between sustainability-driven polymer usage and maintaining structural integrity in high-performance printed components. A deeper understanding of these degradation pathways will inform future guidelines for processing optimization, material compounding, and life-cycle assessment of biobased polymers in the context of sustainable additive manufacturing [1, 15, 14].

2. Materials and Methods

2.1 Polymer Material and Recycling Method

This study investigates a biodegradable, semi-crystalline PLA (Renew® 201, Futerro, Anderlecht, Belgium) with varying thermal histories. The virgin grade has a density ρ of 1.24 g · cm^{-3}, a melting temperature of 175 °C, and a glass transition temperature of 60 °C (according to the supplier). The PLA is processed through six recycling cycles via FGF, starting with virgin material. Before processing, the PLA is dried at 50 °C for 24 h.

After each cycle, the printed parts are mechanically recycled using a RAPID 1514 cutting mill (Rapid Granulator, Bredaryd, Sweden), dried, and reused (cf. Fehler! Verweisquelle konnte nicht gefunden werden.).

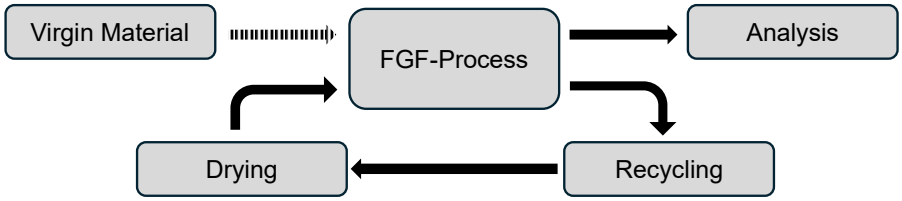

Figure 1: Recycling analysis and manufacturing process route.

2.2 Additive Manufacturing Process

Test specimens are produced by FGF using a Princore MAX printer with granulate extruder (Princore GmbH, Berlin). The printer has a 270 × 375 × 220 mm³ build envelope and uses Klipper firmware. The following machine settings and parameters are used: nozzle diameter 0.4 mm, layer thickness 0.2 mm, extrusion temperature 245 °C, print speed 40 mm·s^{-1} and travel speed 180 mm·s^{-1}. The extrusion factor is adjusted to account for particle morphology changes, but remains fixed across recycling stages. Build jobs are prepared with the software Ultimaker Cura 5.5.0 from Ultimaker (Utrecht, Netherlands). The specimens for the rheological, flexural, and tensile tests are manufactured in separate jobs. For each test method, five specimens are manufactured. Hence, the specimens are manufactured sequentially during the FGF process.

Before printing, the granulate extruder must be calibrated for each material. This is achieved by setting the rotation-distance parameter in the configuration file, which defines the material output per complete motor revolution and controls the volumetric flow rate. Unlike filament systems, screw-based extruders handle loose granulate, so slippage between screw and material can occur, influenced by polymer viscosity and bulk density. Calibration starts with a preset rotation_distance in steps per mm (17.6 for the Princore Max). A fixed filament length l (500 mm) is extruded, and the expected mass m_{erw} is calculated from filament diameter d (ø1.75 mm) and material density ρ. With these values, m_{exp} is 1.4913 g. The actual mass m is then measured, and the rotation_distance is iteratively updated using:

$$rot\_distance = rot\_distance_{-1} \cdot \frac{m}{m_{erw}} \qquad (1)$$

The iterative adjustment continues until the printer extrudes a mass close to the expected value. Three extrusion trials are performed per iteration step to ensure accuracy, and the average mass is used for the calculation.

Due to production-related deposits in the extruder, the extruder screw can become clogged during the FGF process. This is avoided by implementing regular cleaning intervals after every 10 processes.

2.3 Rheological Experiments

Rheological experiments are carried out in shear using a rotational rheometer. (MCR 702e, Anton Paar, Ostfildern, Germany). Cylindrical samples with a diameter of 24 mm and a

thickness of 1 mm are prepared by FGF. The frequency sweeps are carried out at a temperature of 190 °C. The specimens are dried in an oven at 50 °C for 24 h before testing. A time interval of 5 min is chosen for thermal equilibration. An amplitude sweep (1 to 10 %) determines the linear viscoelastic regime at an angular frequency ω of 10 rad · s^{-1}. Frequency sweeps are subsequently performed in the range of angular frequencies from 1 to 100 rad · s^{-1} (starting with the highest frequency) with a strain amplitude of 5 % in the linear viscoelastic regime to determine the storage modulus G', loss modulus G'' and complex viscosity $|\eta^*|$. All tests are carried out in a nitrogen atmosphere.

2.4 Mechanical Experiments

Flexural experiments are conducted using a Dynamic Mechanical Thermal Analyzer (DMTA) (Gabo Eplexor, Netzsch, Selb, Germany). Rectangular samples with a length of 80 mm, a width of 10 mm, and a height of 4 mm are prepared by FGF. Conditioned specimens are tested at environmental conditions (≈ 25 °C) with a testing speed of 2 mm·min^{-1} and in accordance with DIN EN ISO 178. Tensile bars of type 1BA are prepared by FGF. The tensile tests are performed under uniaxial loading using a Shimadzu EZ-SX (Shimadzu, Kyōto, Japan) with a 5 kN force transducer. The crosshead speed used is 1.2 mm · min^{-1}, corresponding to a strain rate of 2 % min^{-1}. The relevant tensile properties are determined in accordance with DIN EN ISO 527-2. Light microscopic analysis of the samples is performed using a VHX-6000 (Keyence, Osaka, Japan). The analysis of discoloration of the specimens is performed using the CIELAB color scale, with particular consideration of the parameters L* (lightness), a* (green–red axis), and b* (yellow–blue axis) index. [20].

3. Results and Discussion

3.1 Additive Manufacturing and Material Recycling

1600 specimens are produced for the investigation and the provision of material. The most significant proportion consisted of flexural bars (approximately 1300), which are crushed after fabrication and used as the starting material for the subsequent iteration stage.

Figure 2 illustrates optical micrographs (VHX-6000, Keyence, Osaka, Japan) of the granules corresponding to successive recycling iterations. The virgin PLA granulate (Figure 2A) exhibits a homogeneous particle morphology. They are predominantly rounded with an average diameter of approximately 3.5 mm. The particle surfaces are uniform and smooth. In contrast, the recycled granulate presented in Figure 2B–F displays a heterogeneous morphology. The particles are primarily irregular in shape, in some cases exhibiting angular contours. Both small particles and larger fragments are present, ranging in size from 0.5 mm to 6 mm. The optical appearance varies between transparent and opaque, with the proportion of opaque particles increasing systematically with the number of recycling cycles. Opacity can be used as an indicator for the presence of crystalline regions. Typically, the light scatters between the boundaries of the amorphous and crystalline regions [21], which leads to less transparency. Based on that, the number of crystalline regions seems to increase with increasing recycling steps. One potential reason could be shorter polymer chains with increasing recycling number, which favor the formation of more crystalline regions [22] and therefore a higher opacity. Frequently recycled particles also show a slight yellowish discoloration. This discoloration is an indicator of thermo-mechanical degradation [23, 9]. Surface characteristics range from smooth to distinctly rough, with localized features attributable to the additive manufacturing process. In some particles, pronounced layer boundaries are visible, resulting from the layer-by-layer deposition during fabrication.

Additionally, Figure 2D and F reveal grid-like patterns, which originate from components where porosity developed within dense infill regions due to under-extrusion.

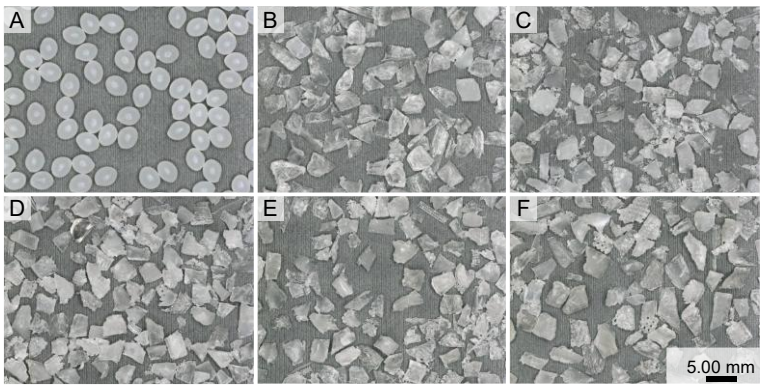

Figure 2: Optical micrographs of the virgin and recycled PLA. A: Iteration 0 - virgin, B: Iteration 1, C: Iteration 2, D: Iteration 3, E: Iteration 4, F: Iteration 5.

The aging behavior and discoloration of the specimen can also be observed in the fabricated test specimens, similar to the findings reported by Romani et al. [15]. When evaluating the specimens, it is also crucial to understand the influence of moisture uptake. Undried and highly recycled samples exhibit a markedly stronger yellowing compared to dried specimens [12]. This effect is also observable in the specimens produced in this study (Figure 3).

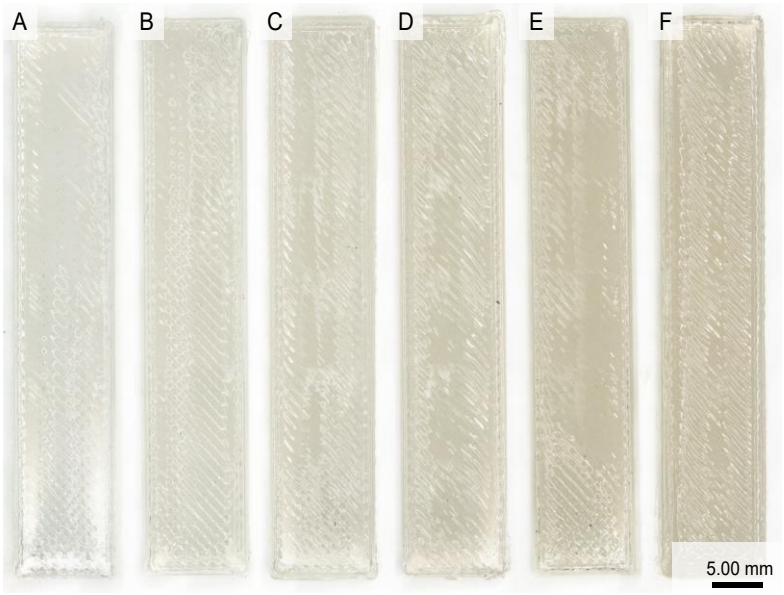

Figure 3: Optical micrographs of the bending specimens. A: Iteration 0 - virgin, B: Iteration 1, C: Iteration 2, D: Iteration 3, E: Iteration 4, F: Iteration 5.

Under processing-related thermal and thermomechanical stresses, chain scissions occur in PLA, leading to a decrease in the average molecular weight, which in turn reduces viscosity, strength, and toughness [13].

The progressive rise in the b* index (Table 1) emphasizes the trend of yellowing across the iteration stages [24].

Table 1: Analysis of the CIELAB b* index.

Iteration	0	1	2	3	4	5
b*	4.969	6.984	8.160	9.843	12.334	12.199

The processing of the material did not reveal any significant abnormalities in general. Each recycling iteration is processable. However, due to diminished flowability, partial material accumulation occurred within the feeding funnel, an effect consistent with previous reports [10]. Adequate feed control was therefore crucial during extrusion. To detect qualitative differences regarding the specimen's shape and quality, recycling iterations 0 and 5 are presented for each type of test specimen as representative examples (Figure 4).

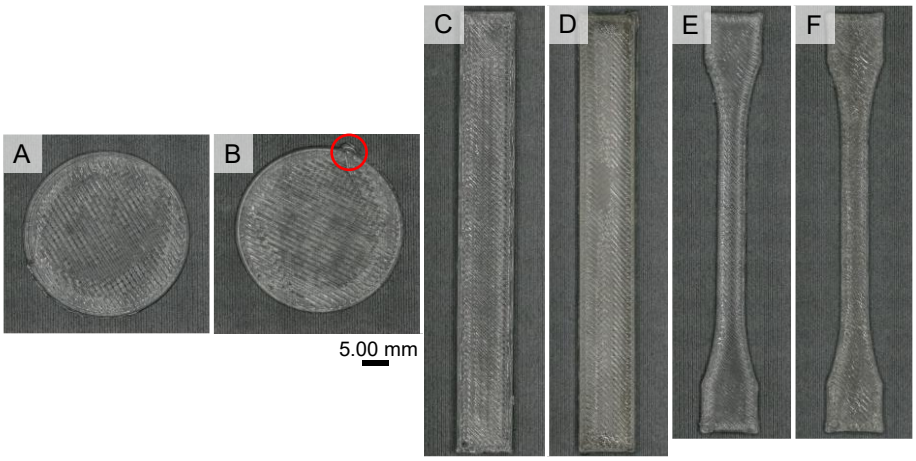

Figure 4: Optical micrographs of the rheological (A, B), flexural (C, D), and tensile specimens (E, F). A, C, E: Iteration 0 - virgin, B, D, F: Iteration 5.

The rheological specimens generally exhibit a circular contour. Local deviations from the ideal circular shape are observable, predominantly occurring in the lowest, initially printed layers. These deviations manifest as thin, wavy protrusions extending beyond the set circular outline. In Figure 4: A, B, a laterally protruding droplet (red circle) of solidified material is also visible. This droplet formed at the end of the printing process when the nozzle completed the toolpath at that position, and a small amount of melt continued to flow before the next specimen was built. That droplet has an approximately length of 3.4 mm and an area of 4 mm^2. Such endpoints are detectable in most samples, either distinctly pronounced, as shown in Figure 4B, or only faintly visible. When comparing the specimens for the flexural experiments (Figure 4: C, D) the rectangular base geometry is clearly identifiable, although minor local contour deviations are apparent, particularly along the side surfaces and corner regions. However, no clear differences regarding the shape between both iterations are visible. The width of the recycled specimens only increases around 2%, whereas thickness decreases around 3%, cross-sectional area around 1% and the specimens mass around 6% compared to the virgin PLA. The surfaces appear generally uneven and exhibit the characteristic line structure associated with additive manufacturing.

Figure 4: E and F present the tensile specimens, allowing the evaluation of geometrical and surface-related characteristics. The contours of the sample generally correspond to the shape specified in the standard; however, minor local deviations are evident. The corners of the tensile bars are not consistently orthogonal and occasionally exhibit rounded protrusions. In the necking region, the contour does not always follow a uniformly smooth curvature. The narrow central section remains approximately parallel over most of its length, while slightly widened regions are primarily observed in the lower, initially printed layers. Compared to the flexural specimens, the deviations between the virgin and five time recycled PLA are larger for the tensile specimens. Overall, the surfaces are non-uniform and display the characteristic line patterns typical of additive manufacturing processes.

3.2 Rheological Properties

For each PLA, the loss modulus G'' is dominant against the storage modulus G' ($G'' > G'$) over the investigated frequency range (Figure 5A). The storage modulus defines the elastic properties of a material. In contrast, the loss modulus defines the energy dissipation due to viscous flow. For the investigation of PLA, the dynamic moduli clearly reveal the slopes 2 and 1 of the Maxwell model in the terminal regime. Hence, the average relaxation time is faster than 10^{-2} s (reciprocal of the frequency at 100 rad $\cdot$ s^{-1}). Based on the short average relaxation time, the macromolecules should be in their equilibrium state directly after deposition [25], which could promote a stronger diffusive/interlayer strength. Note that the data points for G' are only presented for angular frequencies larger than 10 rad $\cdot$ s^{-1}, because with further decreasing frequency, the values of G' leave the tolerance of the rheometer. Furthermore, all PLA show an almost Newtonian behavior with a constant value of complex viscosity over the investigated frequency range (Figure 5B). PLA melts are mainly low-viscous, and the viscosity is not very shear-sensitive [3, 22]. No significant change in the PLA occurs after two recycling steps. The magnitude of the complex viscosity $|\eta^*|$ for the virgin, one-, and two-times recycled PLA is almost identical. The zero-shear rate viscosity η_0 can be determined as ratio of G'' and ω in the terminal zone:

$$\eta_0 = \lim_{\omega \to 0} \frac{G''(\omega)}{\omega} \tag{2}$$

The value for η_0 is approximately 80 Pa $\cdot$ s for the virgin and the first two recycled PLA (Figure 5B and C). The PLA undergoes a change when it is recycled a third time, resulting in a decrease in η_0 of around 18%. The ageing through processing results from the hydrolysis of high molecular chains to lower molecular weight oligomers [3]. A lower molecular weight is associated with shorter polymer chains. This results in a lower melt viscosity [26]. In addition, shorter polymer chains promote a faster formation of crystalline regions [25], favoring warpage during processing. This generally agrees with the observations during FGF processing, where the tendency to warp increases with each recycling step. According to literature, the crystallization kinetics of processed/extruded PLA are substantially faster than for the virgin PLA [16]. The η_0 value decreases even further, when the PLA is recycled for a fourth and fifth time. In these cases, the value of η_0 decreases around 38% compared to the virgin material. The results indicate that the thermal and shear stress during processing affects the rheological properties significantly after two recycling steps, even in FGF. Recent investigations show that for a different PLA, after five recycling steps, the melt viscosity is reduced by about 61% compared to the virgin PLA [15]. If the same recycling route is applied to Fused Layer Modeling (FLM) it may be possible to observe differences even earlier. Since FLM works with filaments, the

manufacturing of the filament leads to additional thermal and shear stresses. However, further investigations are necessary to validate this assumption for the used PLA in the future.

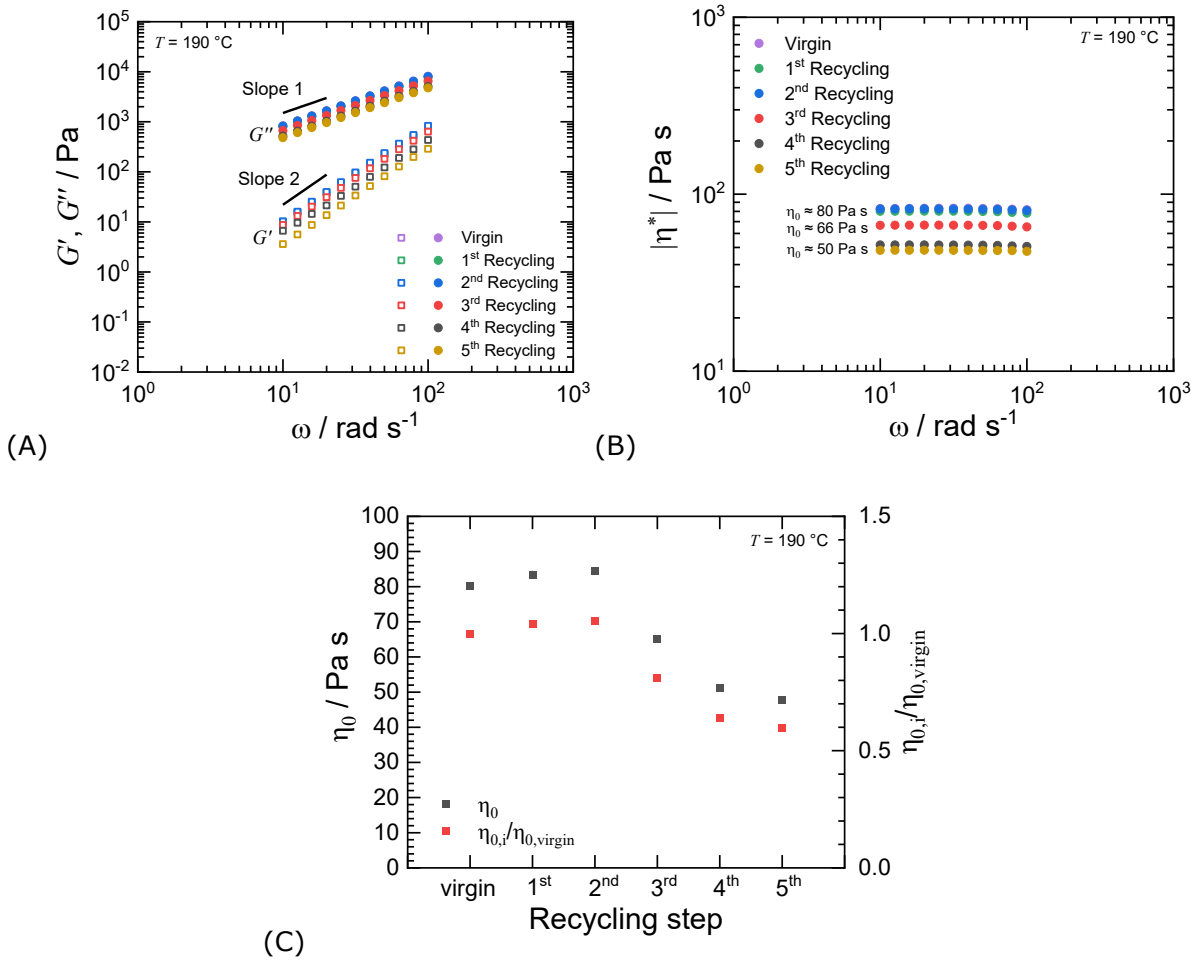

Figure 5: Rheological properties of virgin PLA and after recycling. A: Dynamic moduli G' and G'', B: Complex viscosity $|\eta^*|$ and C: Zero-shear rate viscosity η_0 and normalized data $\frac{\eta_{0,i}}{\eta_{0,virgin}}$.

3.3 Mechanical Properties

To elucidate the underlying recycling mechanisms, tensile and flexural tests are employed. This approach provides a valuable basis for understanding the mechanisms underlying recycling and their influence on the material behavior as a function of the process [10].

Whereas the rheological properties of the virgin and the first two recycling steps are similar, the flexural properties are not (Figure 6A). The virgin PLA shows the highest flexural stress and strain at break. After recycling, these properties decrease until the third recycling step. The flexural stress at break decreases by around 41 % compared to the virgin PLA. After that, a slight increase is observed. This increase could result from the reduced viscosity, which could favor a stronger bonding between adjacent layers and reduce porosity. However, all recycled PLA behave similarly when considering the standard deviation. The manufacturing technique itself could also support this deviation. The FGF machine used is a small-scale machine, and the reproducibility of such machines is often challenging. Manufacturing defects like pores can affect flexural properties significantly. Especially at

low strain rates, where the flexural modulus is determined, the differences between the PLA grades are minor. The flexural modulus only shows slight variation with increasing recycling step (Figure 6B), which is in accordance with previous results. A similar stiffness can be achieved with recycled PLA due to its higher crystallinity [27]. Therefore, some compensation occurs, as the PLA chains shorten with increasing recycling, while the crystallinity increases as a result. Each PLA shows a brittle behavior (breaking of each sample before 2 % strain). In none of the tests, a strain of 5 % was reached (Figure 6C). Overall, degradation occurs, as evidenced by the reduced flexural properties of the recycled PLA, which aligns with the rheological experiments. However, rheological experiments appear to detect degradation more accurately, as the specimen structure (surface and infill) is no longer influenced by the manufacturing technique during the experiments (since the specimen is in a completely molten state).

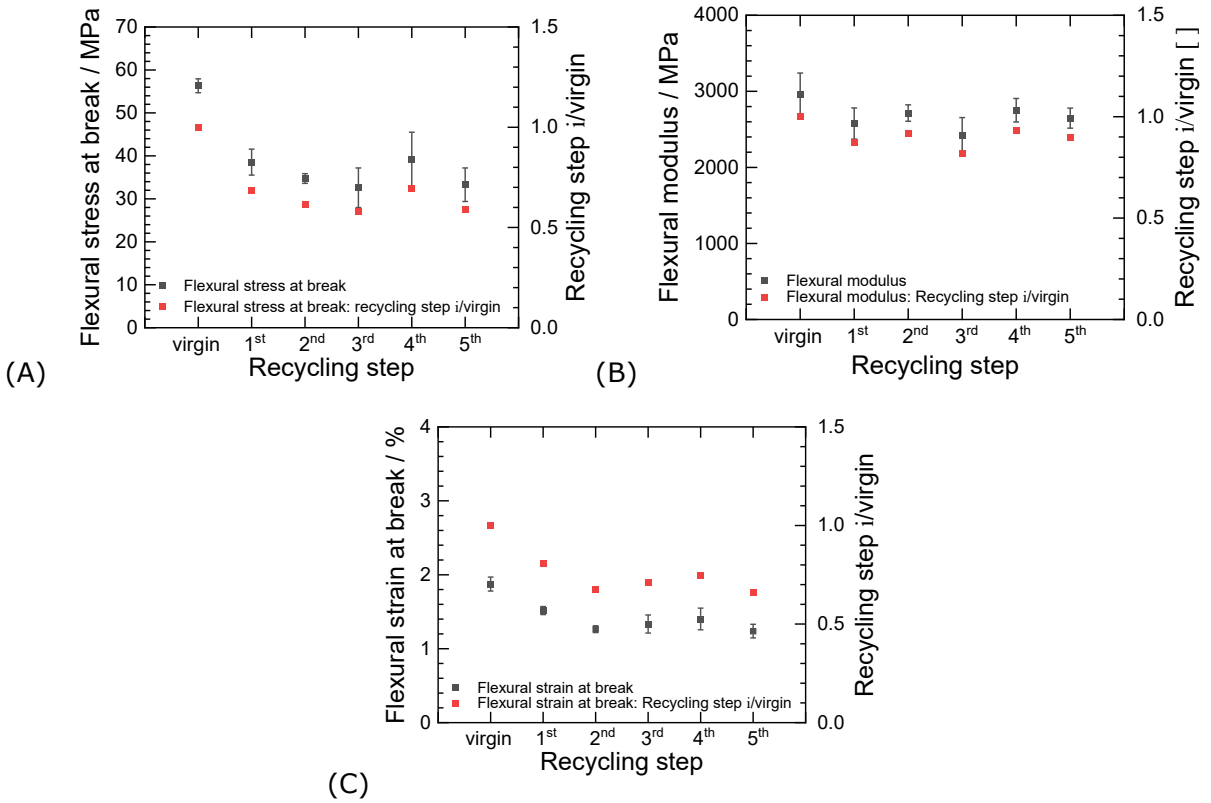

Figure 6: Flexural properties and normalized data of virgin PLA and after recycling. A: Flexural stress at break, B: Flexural modulus, and C: Flexural strain at break.

In addition to the flexural properties, the tensile properties also change from virgin to first recycling of the PLA (Figure 7A-D). Both stress at break and Young's modulus slightly increase from virgin to first recycling. Further recycling reduces these properties even more. The stress at break after five recycling steps is reduced by about 6 % compared to the virgin PLA (Figure 7B). Nevertheless, the Young's modulus of all recycled PLA is still higher than for the virgin PLA (33 % higher after five recycling steps) (**Figure 7C**). An increase of the Young's modulus after some recycling steps was observed in literature, too [15, 23]. When taking the strain at break into account, the trend shows that it decreases with increasing recycling steps (Figure 7D). A more brittle behavior of the specimens could indicate a higher crystallinity. This could explain the increase in the Young's modulus, too. Since crystalline regions are more resistant to deformation due to the intermolecular bonds

in the crystalline phase, the stiffness could increase. This seems more significant for the tensile than for the flexural properties. The overall decrease in the strain at break is around 34 %. However, all specimens show brittle breakage with strain at break values lower than 3 %.

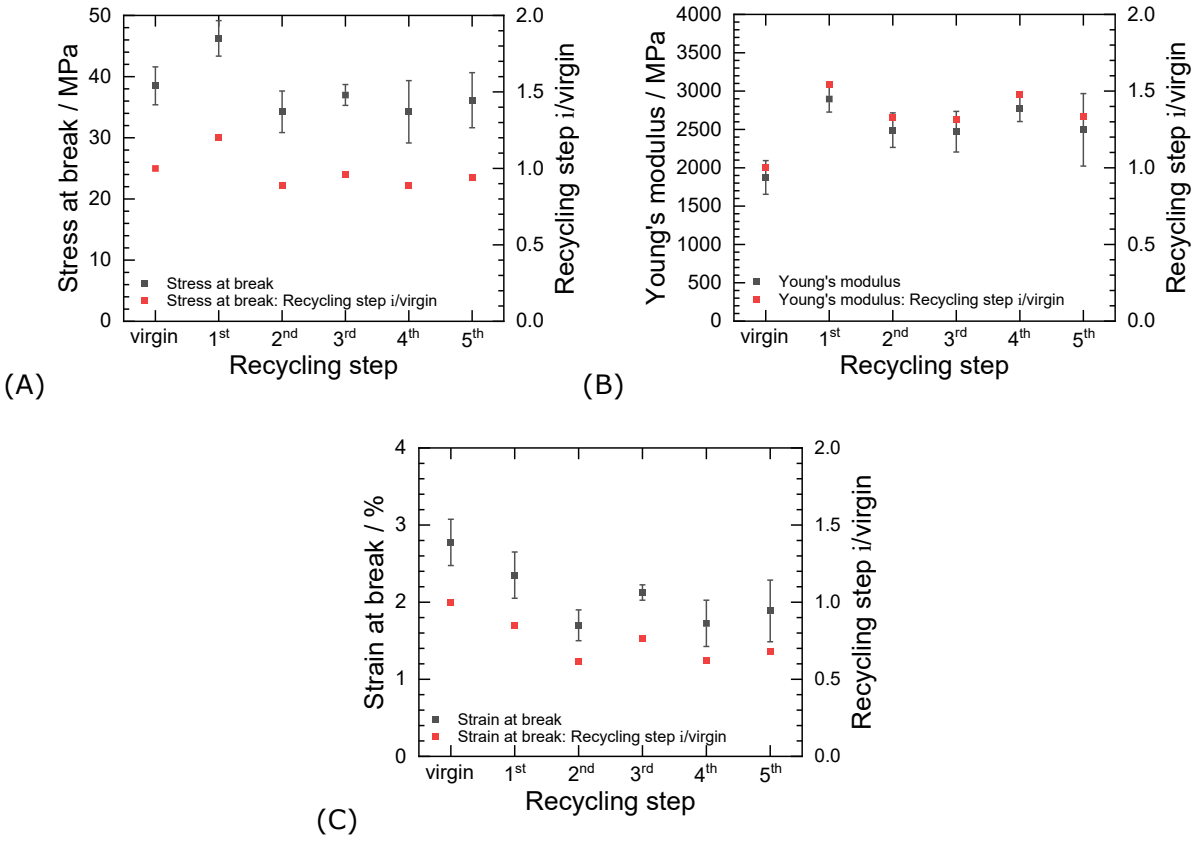

Figure 7: Tensile properties and normalized data of virgin PLA and after recycling. A: Stress at break, B: Young's modulus, and C: Strain at break.

4. Conclusions and Outlook

The results indicate that the PLA exhibits signs of aging throughout the iterative recycling steps. This aging behavior is reflected in rheological measurements and the mechanical analyses. The rheological properties show a distinct evolution with increasing iteration, suggesting progressive structural changes (reduction of chain length) within the material after three recycling iterations. However, the mechanical testing results do not fully corroborate this trend, implying that the intrinsic material properties do not solely govern the mechanical performance. Instead, the findings suggest that the processing conditions and specimen characteristics are more strongly influenced by the material's viscosity than initially anticipated, highlighting the complex interplay between rheological behavior, processing (e.g., interdiffusion of adjacent layers), and mechanical performance. As a subsequent step, the influence of viscosity should be examined in more detail. Furthermore, it would be advisable to replicate this study using an FLM system to identify and compare process-related effects relative to the FGF approach.

5. Acknowledgements

The authors thank Mr. Pascal Brech, Mr. Julian Dührkoop, Mr. Rio Mathias Mungok, and Mr. Julian Maciejok for experimental support.

6. Contributions

L.P.M.B.: Specimen design, Experimental design, methodology, data curation, formal analysis, writing-original draft

C.K.: Specimen design, Experimental design, methodology, data curation, formal analysis, writing-original draft

T.G.: writing-review, and editing

U.A.H.: resources, writing-review and editing, supervision, project administration

J.T.S.: resources, writing-review and editing, supervision, project administration, funding acquisition

All authors: Project Management, technical consultant

References

[1] J. Stanley, D. Culliton, A.-J. Jovani-Sancho et al., “The Journey of Plastics: Historical Development, Environmental Challenges, and the Emergence of Bio-plastics for Single-Use Products,” Eng, vol. 6, p. 17, 2025. doi: 10.3390/eng6010017.

[2] D. Garlotta, “A Literature Review of Poly(Lactic Acid),” Journal of Polymers and the Environment, vol. 9, pp. 63–84, 2001. doi: 10.1023/A:1020200822435.

[3] R. E. Drumright, P. R. Gruber, and D. E. Henton, “Polylactic Acid Technology,” Advanced Materials, vol. 12, pp. 1841–1846, 2000. doi: 10.1002/1521-4095(200012)12:23<1841:AID-ADMA1841>3.0.CO;2-E.

[4] J. E. Lee, D. Lee, J. Lee et al., “Current methods for plastic waste recycling: Challenges and opportunities,” Chemosphere, vol. 370, p. 143978, 2025. doi: 10.1016/j.chemosphere.2024.143978.

[5] G. S. Kanda, I. Al-Qaradawi, and A. S. Luyt, “Morphology and property changes in PLA/PHBV blends as function of blend composition,” Journal of Polymer Research, vol. 25, 2018. doi: 10.1007/s10965-018-1586-3.

[6] M. Bukvić, S. Milojević, S. Gajević et al., “Production Technologies and Application of Polymer Composites in Engineering: A Review,” Polymers, vol. 17, p. 2187, 2025. doi: 10.3390/polym17162187.

[7] L. Fontana, A. Giubilini, R. Arrigo et al., “Characterization of 3D Printed Polylactic Acid by Fused Granular Fabrication through Printing Accuracy, Porosity, Thermal and Mechanical Analyses,” Polymers, vol. 14, p. 3530, 2022. doi: 10.3390/polym14173530.

[8] P. Q. K. Nguyen, J. Panta, T. Famakinwa et al., “Influences of printing parameters on mechanical properties of recycled PET and PETG using fused granular fabrication technique,” Polymer Testing, vol. 132, p. 108390, 2024. doi: 10.1016/j.polymertesting.2024.108390.

[9] F. A. Cruz Sanchez, H. Boudaoud, M. Camargo et al., “Plastic recycling in additive manufacturing: A systematic literature review and opportunities for the circular economy,” Journal of Cleaner Production, vol. 264, p. 121602, 2020. doi: 10.1016/j.jclepro.2020.121602.

[10] S. G. Kirve, J. Kruse, D. Hesse-Hornich et al., “Polymer Recycling and Production of Hybrid Components from Polypropylene and a Thermoplastic Elastomer Using Additive Manufacturing,” Journal of Manufacturing and Materials Processing, vol. 9, p. 175, 2025. doi: 10.3390/jmmp9060175.

[11] N. Vidakis, M. Petousis, L. Tzounis et al., “Sustainable Additive Manufacturing: Mechanical Response of Polypropylene over Multiple Recycling Processes,” Sustainability, vol. 13, p. 159, 2021. doi: 10.3390/su13010159.

[12] L. M. G. Gonçalves, T. R. Rigolin, B. M. Frenhe et al., “On the Recycling of a Biodegradable Polymer: Multiple Extrusion of Poly(Lactic Acid),” Materials Research, vol. 23, 2020. doi: 10.1590/1980-5373-mr-2020-0274.

[13] I. Velghe, B. Buffel, V. Vandeginste et al., “Review on the Degradation of Poly(lactic acid) during Melt Processing,” Polymers, vol. 15, p. 2047, 2023. doi: 10.3390/polym15092047.

[14] Z. Golubović, B. Bojović, S. Kirin et al., “Effect of Aging on Tensile and Chemical Properties of Polylactic Acid and Polylactic Acid-Like Polymer Materials for Additive Manufacturing,” Polymers, vol. 16, p. 1035, 2024. doi: 10.3390/polym16081035.

[15] A. Romani, L. Perusin, M. Ciurnelli et al., “Characterization of PLA feedstock after multiple recycling processes for large-format material extrusion additive manufacturing,” Materials Today Sustainability, vol. 25, p. 100636, 2024. doi: 10.1016/j.mtsust.2023.100636.

[16] T. Hashemi, S. Liparoti, V. Volpe et al., “Analysis of Crystallization Kinetics of PLA Filament for Fused Filament Fabrication,” Macromolecular Materials and Engineering, 2025. doi: 10.1002/mame.202500204.

[17] A. Curmi and A. Rochman, “Screw extrusion fused granulate fabrication: Trends, materials, extruder classification and future development,” Polymer, vol. 330, p. 128459, 2025. doi: 10.1016/j.polymer.2025.128459.

[18] Y. Cao, T. Shao, and W. Zhen, “Early fluorescence tracking of induced degradation pathways on PLA: Deciphering the dominant synergistic effects of water and oxygen at 40 °C,” Polymer Degradation and Stability, vol. 242, p. 111723, 2025. doi: 10.1016/j.polymdegradstab.2025.111723.

[19] P. Q. K. Nguyen, J. Panta, T. Famakinwa et al., “Sustainable fused granulate fabrication: the effects of multiple recycling processes on mechanical properties of recycled polycarbonate,” Materials Today Sustainability, vol. 31, p. 101166, 2025. doi: 10.1016/j.mtsust.2025.101166.

[20] G. Iannuzzi, B. Mattsson, and M. Rigdahl, “Color changes due to thermal ageing and artificial weathering of pigmented and textured ABS,” Polymer Engineering & Science, vol. 53, pp. 1687–1695, 2013. doi: 10.1002/pen.23438.

[21] Y. Lin, E. Bilotti, C. W. Bastiaansen et al., “Transparent semi-crystalline polymeric materials and their nanocomposites: A review,” Polymer Engineering & Science, vol. 60, pp. 2351–2376, 2020. doi: 10.1002/pen.25489.

[22] R. M. Mungok and U. A. Handge, “Compatibilization of poly(lactic acid)/poly(3-hydroxybutyrate-co-hydroxyvalerate) blends using multifunctional epoxy-based chain extender,” Polymer Engineering & Science, vol. 65, pp. 3687–3703, 2025. doi: 10.1002/pen.27242.

[23] F. A. Cruz Sanchez, H. Boudaoud, S. Hoppe et al., “Polymer recycling in an open-source additive manufacturing context: Mechanical issues,” Additive Manufacturing, vol. 17, pp. 87–105, 2017. doi: 10.1016/j.addma.2017.05.013.

[24] “Reversible post-exposure yellowing of weathered polymers,” 2025. [Online]. Available:https://www.sciencedirect.com/science/article/pii/S0141391004000722. Accessed: Oct. 28, 2025.

[25] L. C. Sanchez, C. A. G. Beatrice, C. Lotti et al., “Rheological approach for an additive manufacturing printer based on material extrusion,” The International Journal of Advanced Manufacturing Technology, vol. 105, pp. 2403–2414, 2019. doi: 10.1007/s00170-019-04376-9.

[26] H. Münstedt, “Rheological properties and molecular structure of polymer melts,” Soft Matter, vol. 7, pp. 2273–2283, 2011. doi: 10.1039/c0sm00891e.

[27] T. Ramos-Hernández, J. R. Robledo-Ortíz, M. E. González-López et al., “Mechanical recycling of PLA: Effect of weathering, extrusion cycles, and chain extender,” Journal of Applied Polymer Science, vol. 140, p. 53759, 2023. doi: 10.1002/app.53759.

Kontaktangaben

Luca P. M. Bürgel
Ruhr-Universität Bochum
Lehrstuhl Hybrid Additive Manufacturing
Fakultät Maschinenbau
44801 Bochum
E-Mail: luca.buergel@ruhr-uni-bochum.de
WEB: https://www.ham.ruhr-uni-bochum.de/ham/index.html.de